Distinctive Whole-brain Cell-Types Strongly Predict Tissue Damage Patterns in Eleven Neurodegenerative Disorders

Authors: Veronika Pak[1,2,3], Quadri Adewale[1,2,3], Danilo Bzdok[2,5,6,7], Mahsa Dadar[8], Yashar Zeighami[8], Yasser Iturria-Medina[1,2,3,4,5*]

Affiliations:
[1] *Department of Neurology and Neurosurgery, McGill University, Montreal, Quebec, Canada*
[2] *McConnell Brain Imaging Centre, Montreal Neurological Institute, Montreal, Quebec, Canada*
[3] *Ludmer Centre for Neuroinformatics & Mental Health, Montreal, Quebec, Canada*
[4] *McGill Centre for Studies in Aging, Montreal Quebec, Canada*
[5] *Department of Biomedical Engineering, McGill University, Montreal, Quebec, Canada*
[6] *School of Computer Science, McGill University, Montreal, Quebec, Canada*
[7] *Mila – Quebec Artificial Intelligence Institute, Montreal, Quebec, Canada*
[8] *The Douglas Research Center, Montreal, Quebec, Canada*

* Correspondence to: Yasser Iturria-Medina, 3801 University Street, room NW312, Montreal Neurological Institute and Hospital, McGill University, Montreal, Canada H3A 2B4. yasser.iturriamedina@mcgill.ca. ORCID: https://orcid.org/0000-0002-9345-0347

One Sentence Summary: Major cell-types distinctively associate with spatial vulnerability to tissue loss in eleven neurodegenerative disorders.

Abstract: For over a century, brain research narrative has mainly centered on neuron cells. Accordingly, most whole-brain neurodegenerative studies focus on neuronal dysfunction and their selective vulnerability, while we lack comprehensive analyses of other major cell-types' contribution. By unifying spatial gene expression, structural MRI, and cell deconvolution, here we describe how the human brain distribution of canonical cell-types extensively predicts tissue damage in eleven neurodegenerative disorders, including early- and late-onset Alzheimer's disease, Parkinson's disease, dementia with Lewy bodies, amyotrophic lateral sclerosis, frontotemporal dementia, and tauopathies. We reconstructed comprehensive whole-brain reference maps of cellular abundance for six major cell-types and identified characteristic axes of spatial overlapping with atrophy. Our results support the strong mediating role of non-neuronal cells, primarily microglia and astrocytes, on spatial vulnerability to tissue loss in neurodegeneration, with distinct and shared across-disorders pathomechanisms. These observations provide critical insights into the multicellular pathophysiology underlying spatiotemporal advance in neurodegeneration. Notably, they also emphasize the need to exceed the current neuro-centric view of brain diseases, supporting the imperative for cell-specific therapeutic targets in neurodegeneration.

Keywords: brain canonical cell-types, cellular vulnerability, imaging transcriptomics, structural MRI, Alzheimer's disease, Parkinson's disease, amyotrophic lateral sclerosis, frontotemporal dementia, dementia with Lewy bodies.

Introduction

Neurodegenerative diseases (NDs) are characterised by substantial neuronal loss in the central and peripheral nervous system[1]. In dementia-related conditions like Alzheimer's disease (AD), frontotemporal dementia (FTD), and dementia with Lewy bodies (DLB), neurodegeneration can lead to progressive damage in brain regions related with memory, behaviour, and cognition[2]. Other NDs are thought to primarily affect the locomotor system, including motor neurons in amyotrophic lateral sclerosis (ALS) and nigrostriatal dopaminergic circuitry in Parkinson's disease (PD)[3]. Although each disorder has its own distinct etiology, progression, affected brain areas, and clinical manifestations, transcriptomics analyses support that most of them share molecular and cellular mechanisms[4-7].

While research has been mainly focused on neuronal dysfunction, supporting cells such as astrocytes, microglia, oligodendrocytes, cells of the vascular and peripheral immune systems and their contribution to the disease pathology are gaining more recognition[8-10]. Depending on the disease stage, non-neuronal cells in the brain can play a dual role, both protective and detrimental, by producing neuroprotective and pro-inflammatory factors. Thus, their complex response can have both positive and negative effects on neuronal health and survival. For example, the activation of glial cells can lead to metabolic stress, disruption of the blood-brain barrier, and reduced energy, all of which contribute to increased neuronal death[11-15]. In AD, for example, overproduction of pro-inflammatory cytokines leads to the accumulation of amyloid-β and tau plaques, which are known as the major hallmarks of the disease[12, 16, 17]. This process depends on the innate immune system, which includes microglia and astrocytes[18, 19]. Peripheral interference from systemic inflammation or the gut microbiome can also alter the progression of neuronal loss[20]. Growing evidence suggests that these immune-mediated events is a driving force behind the wide range of NDs[18, 19, 21, 22]. Yet, the exact bases behind how these processes contribute to selective neuronal loss across brain regions remain unclear.

Recent studies have suggested that brain spatial patterns in gene expression are associated with regional vulnerability to some neurodegenerative disorders and their corresponding tissue atrophy distributions[23-26]. Comparison of transcriptomic patterns in middle temporal gyrus across various brain diseases showed cell-type expression signature unique for neurodegenerative diseases[7]. Although single-cell transcriptomics and proteomics analyses have advanced our knowledge of cell-type compositions associated with pathology in neurodegeneration[27-29], these are invariably restricted to a few isolated brain regions, usually needing to be preselected at hand for each specific disease. Due to the invasive nature of tissue acquisition/mapping and further technical limitations for covering extended areas[30], no whole-brain maps for the abundance of cell populations in humans are currently available, constraining the analysis of large-scale cellular vulnerabilities in neurological diseases. Accordingly, how spatial cell-types distributions relate to stereotypic regional damages in neurodegeneration remain largely unclear[31].

Here, we extend previous analysis of cellular-based spatiotemporal vulnerability in neurodegeneration in three fundamental ways. First, we use transcriptomics, structural magnetic resonance imaging (MRI), and advanced cell deconvolution to construct whole-brain reference maps of cellular abundance for six canonical cell-types: neurons, astrocytes, oligodendrocytes, microglia, endothelial cells, and oligodendrocyte precursors. Second, we describe the spatial associations of each

canonical cell-type with atrophy maps from eleven low-to-high prevalent neurodegenerative conditions, including early- and late-AD, PD, FTD, DLB, ALS, tau, and TAR DNA-binding protein 43 (TDP43) pathologies. Third, we identify distinctive cell-cell and disease-disease axes of spatial susceptibility in neurodegeneration, obtaining new insights about across-diseases (dis)similarities in underlying pathological cellular systems. We confirm that non-neuronal cells express substantial vulnerability to tissue loss and spatial brain alterations in most studied neurodegenerative conditions, with distinct and shared across-cells and across-diseases mechanisms. This study aids in unraveling the commonalities across a myriad of dissimilar neurological diseases, while also revealing cell-type specific patterns conferring increased vulnerability or resilience to each examined disorder. For further translation and validation of our findings, all resulting analytic tools and cells abundance maps are shared with the scientific and clinical community.

Results

Multimodal data origin and unification approach

We obtained whole-brain voxel-wise atrophy maps for eleven neurodegenerative conditions, including early- and late-onset Alzheimer's disease (EOAD and LOAD, respectively), Parkinson's disease (PD), amyotrophic lateral sclerosis (ALS), frontotemporal dementia (FTD), dementia with Lewy bodies (DLB) and dementia-related pathologies (presenilin-1, TDP43A, TDP43C, 3RTau, and 4RTau; see *Materials and Methods*, *Disease-specific atrophy maps* subsection)[32, 33]. Pathological diagnosis confirmation was performed for AD and related dementias (DLB, presenilin-1, TDP43A, TDP43C, 3RTau, and 4RTau; [32]), while PD, ALS, and FTD were diagnosed based on clinical and/or neuroimaging criteria[34, 35], with some ALS patients being histologically confirmed *post-mortem*[35]. Change in tissue density in the atrophy maps was previously measured by voxel- and deformation-based morphometry (VBM and DBM; *Materials and Methods*, *Disease-specific atrophy maps* subsection) applied to structural T1-weighted MR images, and expressed as a t-score per voxel (relatively low negative values indicate greater GM tissue loss/atrophy; [36, 37]). All maps are registered to the Montreal Neurological Institute (MNI) brain space [38]. In addition, we obtained bulk transcriptomic data for the adult human brain from the Allen Human Brain Atlas (AHBA)[39]. This included high-resolution coverage of nearly the entire brain, measuring expression levels for over 20,000 genes from 3702 distinct tissue samples of six post-mortem specimens, and detailed structural MRI data (see *Materials and Methods*, *Mapping gene expression data*) [39].

Using previously validated approaches to infer gene expression levels (in AHBA data) at not-sampled brain locations[40], mRNA expression levels were completed for all gray matter (GM) voxels in the standardized MNI brain space[38]. Next, at each GM location, densities for multiple canonical cell-types were estimated using the Brain Cell-type Specific Gene Expression Analysis software (BRETIGEA)[41]. This deconvolution method[41] accurately estimates cell proportions from bulk mRNA for six major cell-types (Fig. 1C): neurons, astrocytes, oligodendrocytes, microglia, endothelial cells, and oligodendrocyte precursor cells (OPCs). Overall, atrophy levels for eleven neurodegenerative disorders and proportion values for six major cell-types were unified at matched and standardized locations (MNI space) covering the brain's whole gray matter (see Fig. 1 for schematic description).

We hypothesized (and tested in next subsections) that brain tissue damages in neurodegenerative disorders are associated with distinctive patterns of cells distributions, with alterations on major cell-types playing a key role on the development of each disorder and representing a direct factor contributing to brain dysfunction.

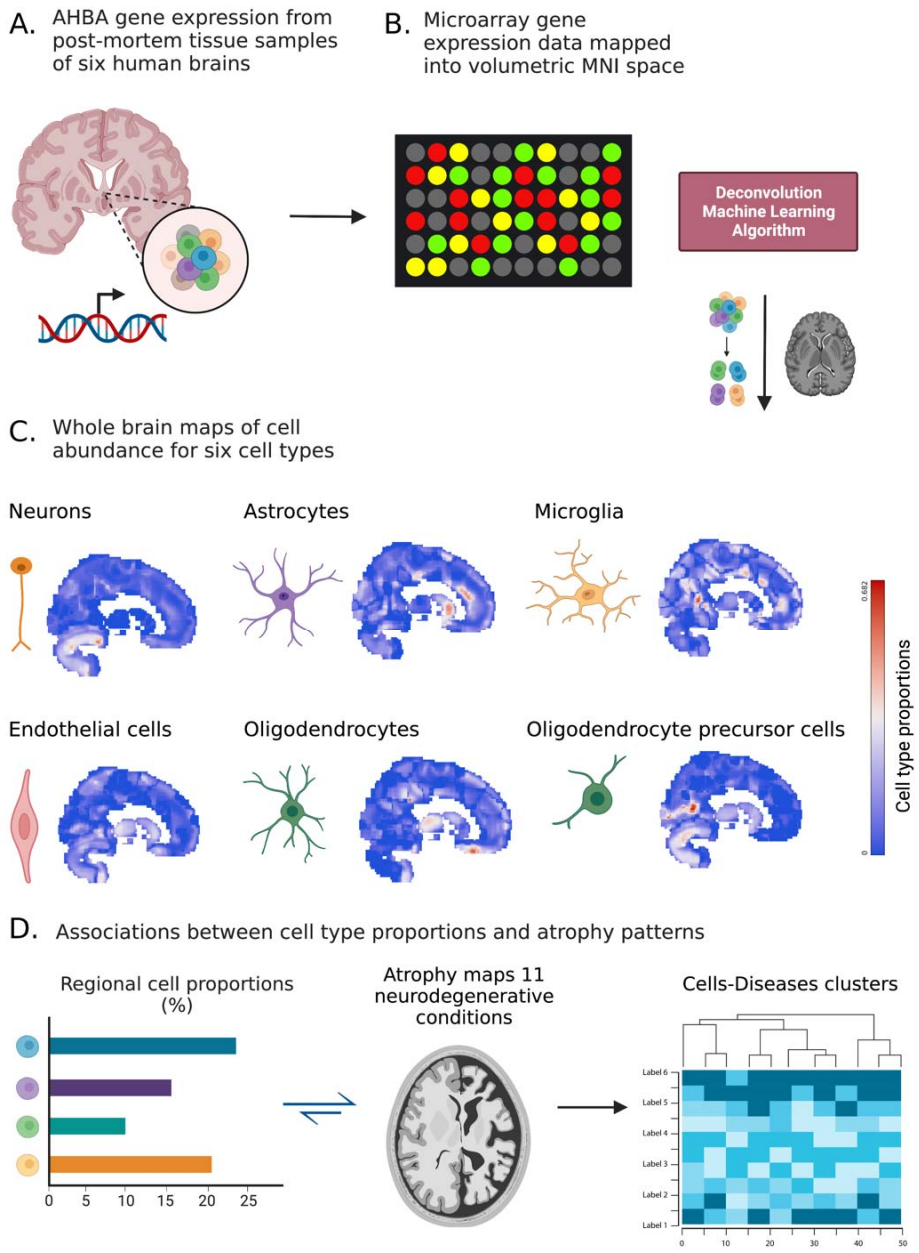

Figure 1 | Schematic approach for whole-brain cells proportions vulnerability analysis in neurodegeneration. (**A**) Gene expression levels in the AHBA were derived from 3072 distinct tissue samples of six post-mortem human brains. (**B**) Microarray gene expression data was inferred for each unsampled GM voxel and together with AHBA data was mapped into volumetric MNI space resulting in the brain-wide transcriptional atlas. Deconvolution machine learning algorithm for bulk RNA expression levels was applied to the transcriptional atlas with using well-known cell-type-specific gene markers. (**C**) Comprehensive volumetric maps showing reconstructed distributions of six canonical cell-types, including neurons, astrocytes, microglia, endothelial cells, oligodendrocytes and OPCs, across all gray

matter voxels in the brain (see *Materials and Methods*, *Cell-type proportion estimation* subsection). At each voxel, red and blue colors indicate high and low proportion densities, respectively. (**D**) Associations between cell-types proportions from each density map and atrophy values in eleven neurodegenerative conditions were analysed in 118 predefined by the AAL atlas regions. Created with BioRender.com

Uncovering spatial associations between cell-type abundances and tissue damage in neurodegeneration

First, we investigated whether stereotypic brain atrophy patterns in neurodegenerative disorders have systematic associations with the spatial distribution of canonical cell-type populations. For each disease and cell-type pair, the non-linear Spearman correlation was calculated with paired atrophy-cell proportion values across 118 cortical and subcortical regions defined by the automated anatomical labelling (AAL) atlas (Table S1; [42]). The results (Figs. 2A-L) show clear associations for all the studied diseases, suggesting extensive cell-types related tissue damage vulnerability in NDs. We confirmed that the observed relationships are independent of brain parcellation, obtaining equivalent results for a different brain parcellation (i.e., DKT atlas [43]; see Fig. S1).

As shown in Figs. 2A-L, astrocytes and microglia cell occurrences presented the strongest spatial associations with atrophy in most neurodegenerative conditions, particularly for EOAD, LOAD, DLB, presenilin-1, 3RTau, 4RTau, TDP43A, TDP43C and FTD (all $P < 0.001$). Astrocytes are involved in neuronal support, extracellular homeostasis, and inflammatory regulation in response to injury, and show high susceptibility to senescence and oxidative damage[44, 45]. Astrocytes also play an important role in the maintenance of the blood-brain barrier (BBB)[46]. Atrophy patterns in cortical regions of genetic FTD was shown to be associated with higher expression of astrocytes- and endothelial cells-related genes[26]. There is evidence of endothelium degeneration and vascular dysfunction in AD and PD[47, 48]. This degeneration may lead to disruption of the BBB, which would allow harmful substances to enter the brain, including inflammatory molecules and toxic aggregated proteins[48, 49]. Furthermore, the endothelium plays a key role in delivering oxygen and nutrients. The disruption of this process in neurodegeneration may lead to impaired brain function and cognitive decline[14, 50].

Similarly involved in neuronal support, microglial cells are the resident macrophages of the central nervous system and key players in the pathology of neurodegenerative conditions including EOAD, LOAD, PD, FTD and ALS[12, 51, 52]. Besides its many critical specializations, microglial activation involvement in prolonged neuroinflammation is of particular relevance in NDs[11,53]. At earlier stages of AD, increased population of microglia and astrocytes (microgliosis and astrogliosis) have been observed in diseased regions, due to sustained cellular proliferation in response to disturbances, loss of homeostasis or the accumulation of Aβ[13, 54, 55]. Excessive proliferation leads to the transition of homeostatic microglia to its senescent or disease-associated type, also called DAM in mice models, via the processes mediated by *TREM2-APOE* signalling[54, 56, 57]. Increased number of dystrophic microglia, a form of cellular senescence characterized as beading and fragmentation of the branches of microglia, has been seen in multiple NDs such as AD, DLB and TDP-43 encephalopathy[58]. The presence of senescent microglia is believed to ultimately contribute to the failure of brain homeostasis and to clinical symptamology[57, 59, 60].

Other non-neuronal cells such as oligodendrocytes and endothelial cells also associated with spatial tissue vulnerability to all NDs aside ALS (Figs. 2J, L). Oligodendrocytes are responsible for the synthesis and maintenance of myelin in the brain[61]. Demyelination produces loss of axonal insulation leading to sensory or motor neuron death in AD and ALS[61, 62]. Oligodendrocytes were shown to be highly genetically associated with PD[63-65] and be particularly vulnerable to the alpha-synuclein accumulation[66, 67]. Mature oligodendrocytes may be in direct contact with the vascular basement membrane, allowing the direct signaling and exchange of substances with endothelial cells[68, 69]. This particular location could underlie specific functions of vasculature-associated oligodendrocytes, which may contribute to the observed oligodendrocytes-mediated tissue vulnerability in NDs[68]. In addition, densities of OPCs showed strong correlations with the atrophy patterns of DLB and TDP43C. OPCs regulate neural activity and harbor immune-related and vascular-related functions[70]. In response to oligodendrocyte damage, OPCs initiate their proliferation and differentiation for the purpose of repairing damaged myelin[71]. In AD, PD and ALS, the OPCs become unable to differentiate and their numbers decrease, leading to a reduction in myelin production and subsequent neural damage[72, 73]. Curiously, depletion of TDP-43 proteins (in TDP-43A&C, FTD and ALS) may provoke the progressive loss of oligodendrocytes and OPCs[74, 75].

We observed (Fig. 2) that neuronal abundance distribution is also associated with tissue damage in many neurodegenerative conditions. However, these associations are less strong than for other cell-types, except for the ALS case (Fig. 2K). For this disorder, neuron proportions positively correlated with tissue integrity (i.e., the higher the neuronal proportion the less atrophy in a region). This observation suggests that increased neuronal presence at brain regions (relative to all considered cell-types) may have a protective effect in ALS, making neuronal enriched regions less vulnerable to damage in this disorder. In addition, we observed particularly weak associations between neuronal proportions and tissue damage in FTD and PD (Fig. 2L), suggesting that these disorders may be primary associated with supportive cell-types (astrocytes and oligodendrocytes, respectively; Figs. 2I, J).

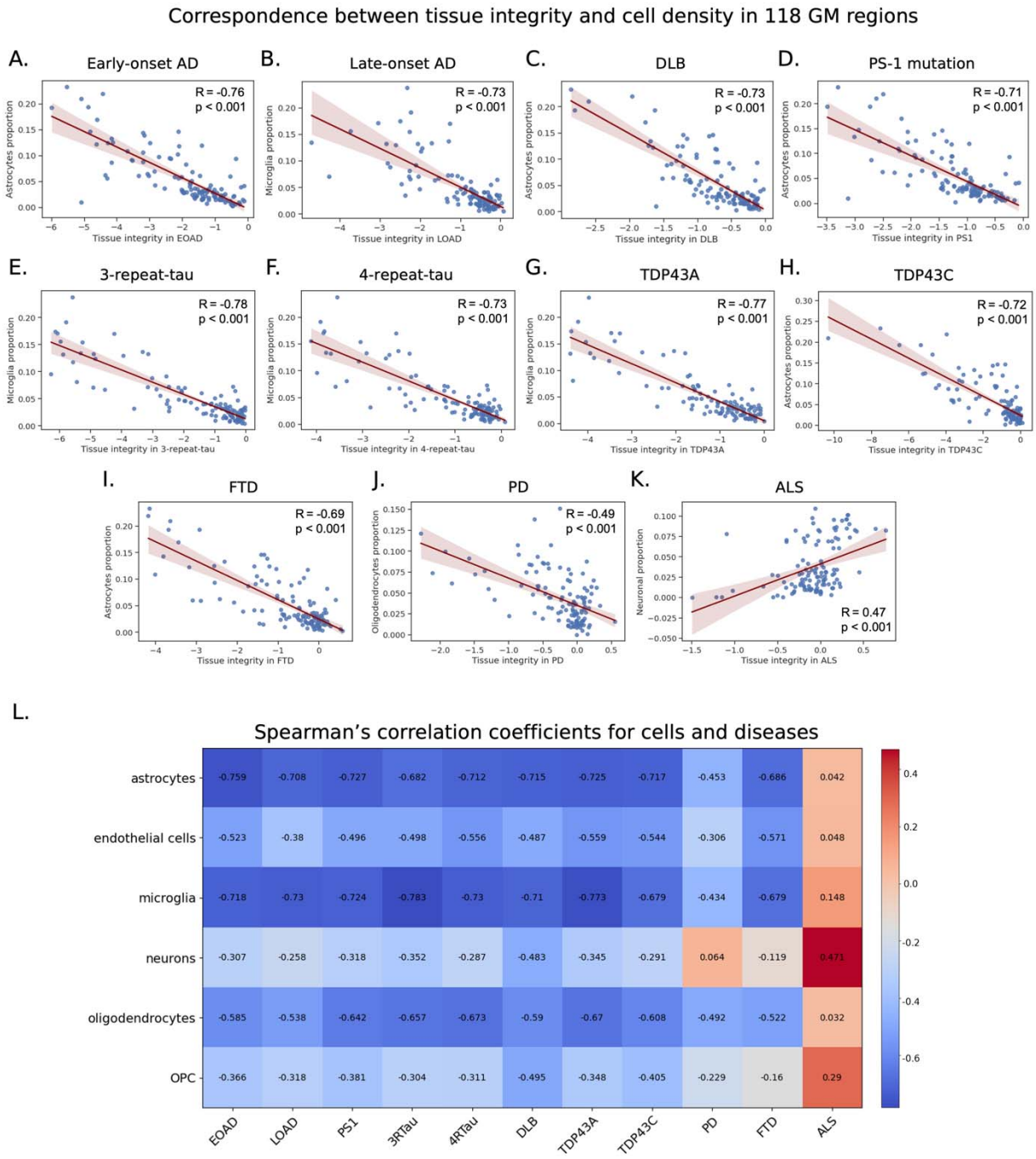

Figure 2 | Spatial associations between tissue integrity and cell-types proportions for eleven neurodegenerative conditions. A-K) Strongest Spearman correlations for EOAD, LOAD, DLB, PS1, 3RTau, 4RTau, TDP43A, TDP43C, FTD, PD, and ALS, respectively. L) All pairwise cells-diseases correlation values. In A-K, each dot represents a GM region from the AAL atlas (Table S1; see Fig. S1 for equivalent results for the DKT parcellation). Lower tissue integrity score indicates greater GM loss/atrophy. Notice how astrocyte density significantly correlates with increase in tissue loss in EOAD, DLB, PS1, TDP43C, and FTD (A, C, D, H, I; $P < 0.001$). Tissue loss was also associated with increase in microglial proportion in LOAD, 3RTau, 4RTau, and TDP43A (B, E, F, G; $P < 0.001$), and increase in oligodendrocytes in PD (J; $p < 0.001$). Increase in neuronal proportion showed association with decrease in atrophy and tissue enrichment in ALS (K; $p < 0.001$).

Spatial cell-types grouping exposes distinctive disease-disease mechanisms.

Next, we hypothesized that diseases sharing similar biological mechanisms and clinical manifestations present common across-brain patterns of cell-types density associations. Figure 3 shows a hierarchical taxonomy dendrogram grouping cell-types and diseases according to their common brain-wide correlation patterns. We observed that AD-related conditions formed its own cluster with other tau pathologies. Also, patterns of cell-types vs tissue loss in both PD and ALS (known for causing major motor symptoms) were distinct compared with the group of dementias, which primary affect cognitive functioning.

Patterns in cellular vulnerability in DLB did not strongly resemble PD without dementia (Fig. 3C), although both conditions involve alpha-synuclein aggregates[76]. This observation supports the hypothesis that clinical deterioration in DLB and PD is not uniquely caused by alpha-synuclein neurodegeneration alone but by distinctive regional spreading patterns[77, 78]. Previously, differences in cell-type-specific gene expression and bulk-tissue samples differential splicing distinguished PD from the Lewy body dementias, with PDD and DLB demonstrating more similarities[64]. Similar observation can be made for ALS and FTD, despite the presence of TDP-43 accumulations in both conditions[79] and their strong genetical overlap[80], they did not group together and with FTLD-tau pathologies (3RTau, 4RTau, TDP43A) based on patterns of cellular vulnerabilities. These results emphasize the fundamental role of network topology (beyond the presence of toxic misfolded proteins) in developing characteristic tissue loss and clinical manifestations in NDs[33, 81-83].

Among all cell-types, neurons and OPCs spatial density distributions were least associated with tissue atrophy in all eleven disorders, subsequently clustering together. Astrocytes and microglia distributions showed the strongest associations with dementia-related pathologies, and thus formed a separate group while still being related with oligodendrocytes and endothelial cells. Astrocytes and microglia are known to be intimately related in the pathophysiological processes of NDs [13]. Both are key regulators of inflammatory responses in the central nervous system, and given their role in clearing misfolded proteins, dysfunctions of each of them can result in the accumulation of Aβ and tau[13, 17]. During the progression of AD and PD, resident microglia undergo proinflammatory activation, resulting in an increased capacity to convert resting astrocytes to reactive astrocytes [84]. Recent studies demonstrated that blocking the microglial-mediated conversion of astrocytes to a neurotoxic reactive phenotype could limit neurodegeneration in AD and PD[84, 85].

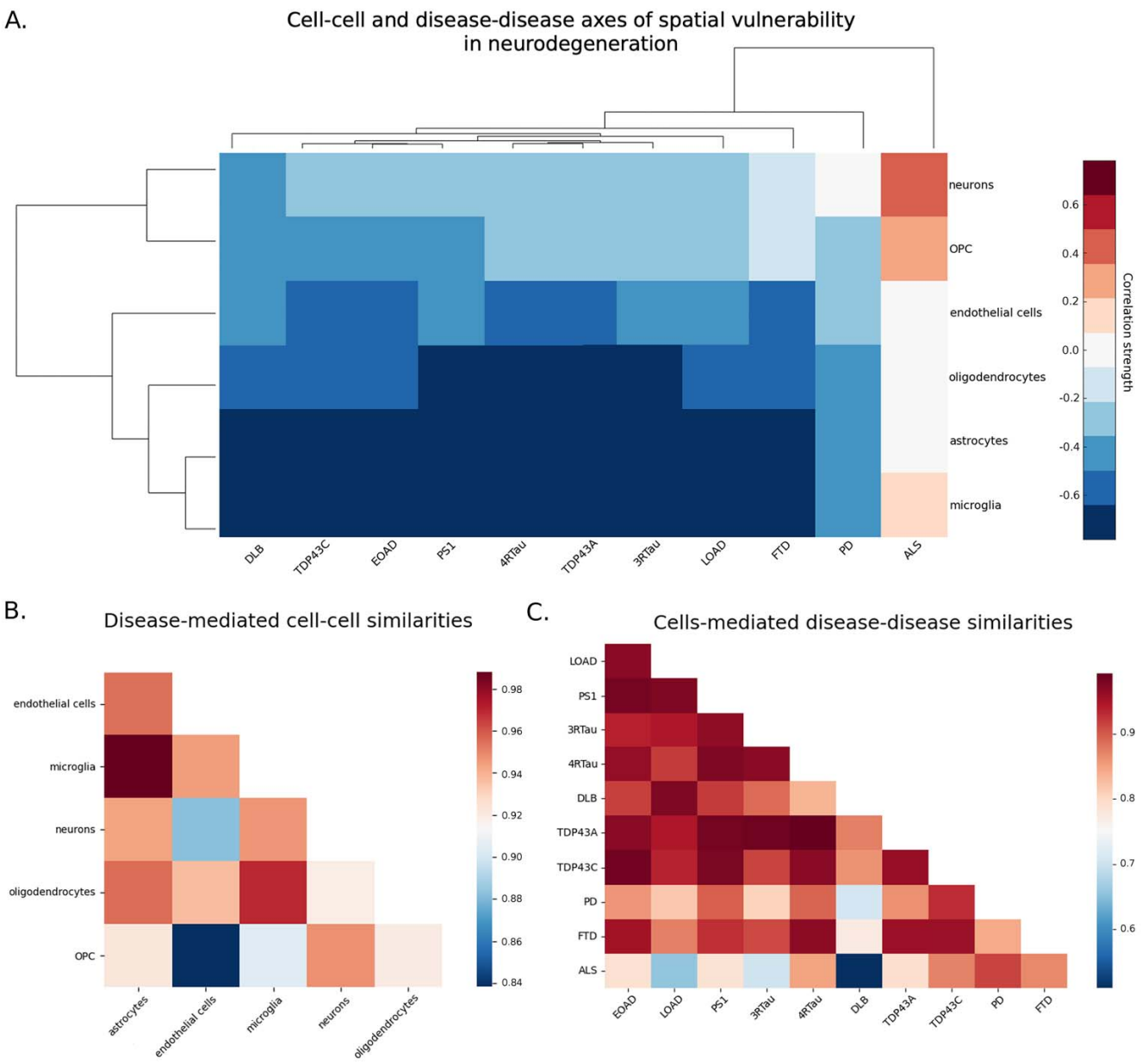

Figure 3 | Cells and diseases similarities based on shared distributions. A) Dendrogram and unsupervised hierarchical clustering heatmap of Spearman's correlations between cell-type proportions and atrophy patterns of the eleven neurodegenerative diseases. B) Cell-cell associations based on regional vulnerabilities to tissue loss across neurodegenerative conditions. C) Disease-disease similarities across cell-types. In A), red color corresponds to strong positive correlations between cells and diseases, white to no correlation, and dark blue to strong negative correlation.

Discussion

Previous efforts to describe the composition of the brain's different cell populations related to neurodegeneration have been limited to a few isolated regions. In the most systematic study of its kind, here we characterized large-scale spatial associations between canonical cell-types and brain tissue loss

across all cortical and subcortical gray matter areas in eleven neurodegenerative disorders (including early- and late-AD, PD, FTD, DLB, ALS, tauopathies). Starting from gene expression and structural MRIs from the Allen Human Brain Atlas[39], and extending our analysis with advanced RNAseq cells deconvolution approaches and whole-brain atrophy maps from clinically and/or neuropathologically confirmed diseases. We determined that (i) the spatial distributions of non-neuronal cell-types, primarily microglia and astrocytes, are strongly associated with the spread tissue damage present in many neurodegenerative disorders; (ii) cells and diseases define major axes that underlie spatial vulnerability according with shared cellular mechanisms, which aid in comprehending heterogeneity behind distinct and similar clinical manifestations/definitions; (iii) the generated whole-brain maps of cellular abundance can be similarly used for studying cellular processes in other neurological conditions (e.g., neurodevelopmental and neuropsychiatric disorders). Overall, our findings stress the critical need to surpass the current neuro-centric view of brain diseases and the imperative for identifying cell-specific therapeutic targets in neurodegeneration[59]. For further translation and validation, all resulting cells abundance maps and analytic tools are freely shared with the community.

We derived, first to our knowledge, high resolution maps of cellular abundance/proportion in the adult human brain for six canonical cell-types, including astrocytes, neurons, oligodendrocytes, microglia, and endothelial cells. As mentioned, previous cellular analyses of neurological conditions have been restricted to expert-selected isolated brain areas. The invasive nature of expression assays, requiring direct access to neural tissue, and other numerous scaling limitations have impeded extensive spatial analyses[86]. Earlier studies, also using AHBA data, have shown that spatial patterns in gene expression and cell-type-specific genetic markers are associated with both regional vulnerability to neurodegeneration and patterns of atrophy across the brain[7, 23-26]. Since many neurodegeneration-related genes have similar levels of expression in both affected and unaffected brain areas[87], characterizing changes in tissue loss associated with cell-type proportions may provide a clearer perspective on large-scale spatial patterns of cellular vulnerability. Our maps of cells-abundance are available for the scientific and clinical community, potentially allowing researchers to further study spatial variations in cell-types density with macroscale phenotypes. These maps can be used in future studies concerning brain structure and function in both health and disease. They can be also explored in context of other neurological diseases including neurodevelopmental and psychiatric conditions.

Our results demonstrate that all canonical cell-types express vulnerability to dementia-related atrophy of brain tissue, suggesting the disruption of the molecular pathways involving specific cell-types can contribute to their observed dysfunctions and subsequent clinical symptamology[59]. Previously, transcriptional profiling of prefrontal cortex in AD showed reduced proportions of neurons, astrocytes, oligodendrocytes, and homeostatic microglia[88]. In contrast, bulk-RNA analysis of diseased AD tissues from various human brain regions observed neuronal loss and increased cell abundance of microglia, astrocytes, and oligodendrocytes[89, 90]. Furthermore, increased microglial, endothelial cells, and oligodendrocytes population was observed in PD and other Lewy diseases[64, 91]. Cortical regions exhibiting the most severe atrophy in FTD showed increased gene expression of astrocytes and endothelial cells[26]. In line with these results, we observed that regions with increased cell-type proportions, particularly for astrocytes and microglia, are more vulnerable to tissue atrophy in almost all neurodegenerative conditions. This may partly explain the reported cellular proliferation through microglial activation in diseased regions in response to the misfolded protein accumulation or other

pathobiological processes[54, 60]. As disease progresses, the release of inflammatory agents by sustained microglial activation is believed to be responsible for exacerbating neurodegeneration and clinical symptoms[18, 21]. Microglial activation in pair with gray matter atrophy in frontal cortex were shown to be directly associated with cognitive decline in FTD[52].

Taken together, our findings support genome-wide association and transcriptional studies suggesting that cell-type-specific alterations in NDs may indicate the disruption of the following distinct and overlapping molecular pathways: inflammation, immune response, and homeostasis (astrocytes and microglia), vascular system (endothelial cells), and myelination (oligodendrocytes and OPCs)[88, 92-94]. Recent study identified a degree of similarities (grouping) in cell-type expression between AD, FTD, and ALS, distinguishing them from other neurological disorders[7]. Interestingly, our results showed all dementia conditions were similar in their patterns of cell-types associations with tissue loss relative to PD and ALS. AD-associated changes in cell-types proportions were previously suggested to be related to the presence of dementia, not to plaques and tangles[95]. There were no strong similarities in patterns of vulnerabilities between pairs of conditions (PD without dementia and DLB, FTD and ALS) with associated genetic risks and type of toxic proteins[76, 79, 80]. These results reinforce our statement on gray matter atrophy patterns in NDs being not uniquely provoked by genes and misfolded proteins toxicity alone but affected and mediated by additional factors such as metabolic and vascular dysregulations[81, 96-98].

Our study also has a number of limitations. First, our analyses were focused on stereotypic atrophy patterns for each disorder. It is known that NDs are highly heterogenous, with molecular, phenotypic, and clinical subtypes potentially varying in atrophy patterns[99, 100]. Further investigation of cell-type signatures across various subtypes and disease stages may better characterize each case. Similarly, it has been observed that cell-type-related transcriptional changes are different between sexes[70], making future sex-specific analyses indispensable for further understanding of sex-related pathomechanisms. Examined atrophy maps were coming from different studies (Table S2), with differences in data acquisition protocols (e.g., spatial resolution) and technical procedures (e.g., smoothing level, statistical methods). In complementary analyses, we observed almost identical results after smoothing all disease-specific images with the same kernel size, while they were already mapped at the same spatial resolution for this study and statistically adjusted by acquisition parameters (e.g., field strength) in original studies. Cell-types deconvolution approaches are varied and limited in their precision[101]. Here, we used a previously validated deconvolution method designed for efficiently estimating cell proportions for six major cell-types from bulk mRNA expression [41]. Conveniently, this method is freely available for researchers (R package, BRETIGEA), which will facilitate reproducibility analyses of our study. Other important considerations are the dynamic nature of gene expression as disease progresses[102, 103], *post-mortem* RNA degradation of the used templates [104], and the subsequent limited ability of bulk RNA sequencing to reflect cell-to-cell variability, which is relevant for understanding cell heterogeneity and the roles of specific cell populations in disease [105]. Lastly, a promising future direction would be to validate our findings with single-cell spatial analyses alongside cellular interaction modeling with pluripotent stem (iPS) cells.

Materials and Methods

Disease-specific atrophy maps. Voxel-wise brain atrophy maps in early- and late-onset Alzheimer's disease (EOAD and LOAD), Parkinson's disease (PD), amyotrophic lateral sclerosis (ALS), frontotemporal dementia (FTD), dementia with Lewy bodies (DLB) and dementia-related pathologies (presenilin-1, TDP43A, TDP43C, 3RTau, and 4RTau) were adopted from open data repositories and/or requested from collaborators[32, 33], as specified below. Reduction in gray matter (GM) density in diseased atrophy maps relative to controls was measured by voxel- and deformation-based morphometry (VBM and DBM) applied to structural T1-weighted MR images, and thus were expressed as t-score per voxel (relatively low negative t-scores indicate greater GM tissue loss/atrophy)[36, 37]. VBM is a hypothesis-free technique for analyzing neuroimaging data that characterizes regional tissue concentration differences across the whole brain, without the need to predefine regions of interest[106]. DBM is a similar widely used technique to identify structural changes in the brain across participants, which in addition considers anatomical differences such as shape and size of brain structures[107]. See Table S2 for study-origin, sample size and imaging technique corresponding to each atrophy map.

MRI data for neuropathological dementias were collected from 186 individuals and averaged across participants per condition: 107 had a primary AD diagnosis (68 early-onset (<65 years at disease onset), 29 late onset (≥65 years at disease onset), 10 presenilin-1 mutation carriers), 25 with DLB, 11 with 3-repeat-tau, 17 with 4-repeat-tau, 12 TDP43A, and 14 TDP43C)[32]. Data were collected from multiple centres on scanners from three different manufacturers (Philips, GE, Siemens), using a variety of different imaging protocols[32]. Magnetic field strength varied between 1.0 T (n=15 scans), 1.5 T (n=201 scans) and 3 T (n=43 scans)[32]. Atrophy maps were statistically adjusted for age, sex, total intracranial volume, and MRI strength field and site[32]. Ethical approval for this retrospective study was obtained from the National Research Ethics Service Committee London-Southeast[32].

MRI data for PD, consisted of 3T high-resolution T1-weighted scans, were obtained from the Parkinson's Progression Markers Initiative (PPMI) database (www.ppmiinfo.org/data). The PPMI is a multi-center international study with approved protocols by the local institutional review boards at all 24 sites across the US, Europe, and Australia[83]. MRI and clinical data used in constructing atrophy maps were collected from 232 participants with PD[83]. PD subjects (77 females; age 61.2 ± 9.1) were required to be at least 30 years old or older, untreated with PD medications within 2 years of diagnosis, and to display at least two or more PD-related motor symptoms[83]. No significant effect of age, gender, or site was found[83].

For ALS, MRI data was collected from 66 patients (24 females; age 57.98 ± 10.84) with both sporadic or familial form of disease from centers of the Canadian ALS Neuroimaging Consortium (http://calsnic.org/, ClinicalTrials.gov NCT02405182), which included 3T MRI sites in University of Alberta, University of Calgary, University of Toronto, and McGill University[108]. All participants gave written informed consent, and the study was approved by the health research ethics boards at each of the participating sites[108]. Participants were excluded if they had a history of other neurological or psychiatric disorders, prior brain injury or respiratory impairment resulting in an inability to tolerate the MRI protocol[108]. Normative aging as well as sex differences were regressed out from data prior the map construction[108].

For FTD, MRI data was accessed from the frontotemporal lobar degeneration neuroimaging initiative (FTLDNI), which included 125 patients (73 females, age 63.52 ± 7.03) with frontotemporal dementia diagnosis[109]. 3T structural images were collected on three following sites: University of California San Francisco, Mayo Clinic, and Massachusetts General Hospital[109]. All subjects provided informed consent and the protocol was approved by the institution review board at all sites[109]. For up-to-date information on participation and protocol, please visit: http://memory.ucsf.edu/research/studies/nifd.

Mapping gene expression data. To construct a comprehensive transcriptome atlas, we used RNA microarray gene expression data from the Allen Human Brain Atlas (AHBA; https://human.brain-map.org/)[39]. The AHBA included anatomical and histological data collected from six healthy human specimens with no known neurological disease history (one female; age range 24–57 years; mean age 42.5 ± 13.38 years)[39]. Two specimens contained data from the entire brain, whereas the remaining four included data from the left hemisphere only, with 3702 spatially distinct samples in total[39]. The samples were distributed across cortical, subcortical, brainstem and cerebellar regions in each brain, and quantified the expression levels of more than 20,000 genes[39]. mRNA data for specific brain locations were accompanied by structural MR data from each individual and were labeled with Talairach native coordinates and Montreal Neurological Institute (MNI) coordinates, which allowed us to match samples to imaging data.

Following the validated approach in [40], missing data points between samples for each MNI coordinate were interpolated using Gaussian-process regression, a widely used method for data interpolation in geostatistics. MNI coordinates for missing mRNA values were taken from the GM regions of the AAL atlas. Spatial covariance between coordinates from 3072 AHBA tissue samples and coordinates from the AAL atlas was estimated via the quadratic exponential kernel function. mRNA expression at each MNI coordinate was then predicted by multiplying AHBA gene express values that corresponded to specific probes to kernel covariance matrix divided by the sum of kernels.

Cell-type proportion estimation. Densities for multiple canonical cell-types were estimated at the gray matter (GM) by applying an R-package Brain Cell-type Specific Gene Expression Analysis (BRETIGEA), with known genetic markers to the transcriptome atlas[41]. This deconvolution method was designed for estimating cell proportions in bulk mRNA expression data for six major cell-types: neurons, astrocytes, oligodendrocytes, microglia, endothelial cells, and oligodendrocyte precursor cells[41]. We chose 15 representative gene markers per each cell-type (90 in total) from the BRETIGEA human brain marker gene set and then selected those genes that were also present in the AHBA gene expression database with matching gene probes. This resulted in eighty cell-type-related gene markers that were used in missing data interpolation and the deconvolution and proportion estimation analysis (Table S3). For each voxel, each cell-type proportion value was normalized relative to the sum of all six cell-types and the sum was scaled relative to the gray matter density. We then registered data into MNI and volumetric space using the ICBM152 template[38].

For the correlation analysis, cell densities were averaged over 118 anatomical regions in gray matter defined by the extended automated anatomical labelling atlas (AAL; Table S1)[42]. We repeated the correlation analysis for the 98 regions from the Desikan-Killiany-Tourville atlas (DKT; Fig. S1)[43].

Data analysis. We constructed a 6 × 11 correlation matrix by computing inter-regional Spearman's correlations between spatial distributions of the six canonical cell-types and patterns of atrophy in eleven neurodegenerative conditions. Shapiro-Wilk tests were used to examine the normality of data distribution. Hierarchical clustering analyses was applied using in-built MATLAB function for data visualization. Samples were clustered together based on estimated averaged linkage Euclidian distance between them.

Data and materials availability: All data needed to evaluate the conclusions in the paper are present in the paper and/or the Supplementary Materials. The BRETIGEA R package can be downloaded from https://cran.r-project.org/package=BRETIGEA. The Allen Human Brain Atlas data is available at https://human.brain-map.org/static/download. Atrophy maps for pathologically confirmed dementia are available at http://neurovault.org/collections/ADHMHOPN/. Raw demographic and MRI data from PD and ALS patients can be accessed at www.ppmiinfo.org/data and http://calsnic.org/ (ClinicalTrials.gov NCT02405182), respectively. We anticipate that resulting cells abundance maps will be freely shared with the community with article publication (at our lab's GitHub space https://github.com/neuropm-lab).

Acknowledgments: This project was undertaken thanks in part to the following funding awards to YIM: the Canada Research Chair tier 2, the CIHR Project Grant 2020, the Weston Family Foundation's Transformational Research in AD 2020, and the New Investigator start-up grant from McGill University's *Healthy Brains for Healthy Lives Initiative* (HBHL, *Canada First Research Excellence Fund*). First author VP was partly supported by HBHL's Theme 1 Discovery fund 2022-2025. In addition, we used the computational infrastructure of the McConnell Brain Imaging Center at the Montreal Neurological Institute, supported in part by the *Brain Canada Foundation*, through the *Canada Brain Research Fund*, with the financial support of *Health Canada* and sponsors.

Competing interests: The authors declare no competing interest.

References

1. Gorman AM. Neuronal cell death in neurodegenerative diseases: recurring themes around protein handling. J Cell Mol Med 2008;12:2263-2280.
2. Duong S, Patel T, Chang F. Dementia: What pharmacists need to know. Can Pharm J (Ott) 2017;150:118-129.
3. Bosco DA, LaVoie MJ, Petsko GA, Ringe D. Proteostasis and movement disorders: Parkinson's disease and amyotrophic lateral sclerosis. Cold Spring Harb Perspect Biol 2011;3:a007500.
4. Wingo TS, Liu Y, Gerasimov ES, et al. Shared mechanisms across the major psychiatric and neurodegenerative diseases. Nat Commun 2022;13:4314.
5. Huseby CJ, Delvaux E, Brokaw DL, Coleman PD. Blood RNA transcripts reveal similar and differential alterations in fundamental cellular processes in Alzheimer's disease and other neurodegenerative diseases. Alzheimers Dement 2022.
6. Arneson D, Zhang Y, Yang X, Narayanan M. Shared mechanisms among neurodegenerative diseases: from genetic factors to gene networks. J Genet 2018;97:795-806.
7. Zeighami Y, Bakken TE, Nickl-Jockschat T, et al. A comparison of anatomic and cellular transcriptome structures across 40 human brain diseases. PLoS Biol 2023;21:e3002058.
8. Bordone MC, Barbosa-Morais NL. Unraveling Targetable Systemic and Cell-Type-Specific Molecular Phenotypes of Alzheimer's and Parkinson's Brains With Digital Cytometry. Front Neurosci 2020;14:607215.
9. Lee H, Fenster RJ, Pineda SS, et al. Cell Type-Specific Transcriptomics Reveals that Mutant Huntingtin Leads to Mitochondrial RNA Release and Neuronal Innate Immune Activation. Neuron 2020;107:891-908 e898.
10. Reynolds RH, Botia J, Nalls MA, et al. Moving beyond neurons: the role of cell type-specific gene regulation in Parkinson's disease heritability. NPJ Parkinsons Dis 2019;5:6.
11. Wareham LK, Liddelow SA, Temple S, et al. Solving neurodegeneration: common mechanisms and strategies for new treatments. Mol Neurodegener 2022;17:23.
12. Guzman-Martinez L, Maccioni RB, Andrade V, Navarrete LP, Pastor MG, Ramos-Escobar N. Neuroinflammation as a Common Feature of Neurodegenerative Disorders. Front Pharmacol 2019;10:1008.
13. Kwon HS, Koh SH. Neuroinflammation in neurodegenerative disorders: the roles of microglia and astrocytes. Transl Neurodegener 2020;9:42.
14. Kalaria RN. The blood-brain barrier and cerebrovascular pathology in Alzheimer's disease. Ann N Y Acad Sci 1999;893:113-125.
15. Chen X, Guo C, Kong J. Oxidative stress in neurodegenerative diseases. Neural Regen Res 2012;7:376-385.
16. Kinney JW, Bemiller SM, Murtishaw AS, Leisgang AM, Salazar AM, Lamb BT. Inflammation as a central mechanism in Alzheimer's disease. Alzheimers Dement (N Y) 2018;4:575-590.
17. Leyns CEG, Holtzman DM. Glial contributions to neurodegeneration in tauopathies. Mol Neurodegener 2017;12:50.
18. Maccioni RB, Rojo LE, Fernández JA, Kuljis RO. The role of neuroimmunomodulation in Alzheimer's disease. Ann N Y Acad Sci 2009;1153:240-246.
19. Zang X, Chen S, Zhu J, Ma J, Zhai Y. The Emerging Role of Central and Peripheral Immune Systems in Neurodegenerative Diseases. Front Aging Neurosci 2022;14:872134.
20. Sochocka M, Donskow-Łysoniewska K, Diniz BS, Kurpas D, Brzozowska E, Leszek J. The Gut Microbiome Alterations and Inflammation-Driven Pathogenesis of Alzheimer's Disease-a Critical Review. Mol Neurobiol 2019;56:1841-1851.
21. Kempuraj D, Thangavel R, Natteru PA, et al. Neuroinflammation Induces Neurodegeneration. J Neurol Neurosurg Spine 2016;1.

22. Castellani G, Croese T, Peralta Ramos JM, Schwartz M. Transforming the understanding of brain immunity. Science 2023;380:eabo7649.
23. Vidal-Pineiro D, Parker N, Shin J, et al. Cellular correlates of cortical thinning throughout the lifespan. Sci Rep 2020;10:21803.
24. Roshchupkin GV, Adams HH, van der Lee SJ, et al. Fine-mapping the effects of Alzheimer's disease risk loci on brain morphology. Neurobiol Aging 2016;48:204-211.
25. Zheng YQ, Zhang Y, Yau Y, et al. Local vulnerability and global connectivity jointly shape neurodegenerative disease propagation. PLoS Biol 2019;17:e3000495.
26. Altmann A, Cash DM, Bocchetta M, et al. Analysis of brain atrophy and local gene expression in genetic frontotemporal dementia. Brain Commun 2020;2.
27. Cuevas-Diaz Duran R, González-Orozco JC, Velasco I, Wu JQ. Single-cell and single-nuclei RNA sequencing as powerful tools to decipher cellular heterogeneity and dysregulation in neurodegenerative diseases. Front Cell Dev Biol 2022;10:884748.
28. Luquez T, Gaur P, Kosater IM, et al. Cell type-specific changes identified by single-cell transcriptomics in Alzheimer's disease. Genome Med 2022;14:136.
29. Riley BE, Gardai SJ, Emig-Agius D, et al. Systems-based analyses of brain regions functionally impacted in Parkinson's disease reveals underlying causal mechanisms. PLoS One 2014;9:e102909.
30. Arnatkeviciute A, Fulcher BD, Bellgrove MA, Fornito A. Imaging Transcriptomics of Brain Disorders. Biol Psychiatry Glob Open Sci 2022;2:319-331.
31. Mrdjen D, Fox EJ, Bukhari SA, Montine KS, Bendall SC, Montine TJ. The basis of cellular and regional vulnerability in Alzheimer's disease. Acta Neuropathol 2019;138:729-749.
32. Harper L, Bouwman F, Burton EJ, et al. Patterns of atrophy in pathologically confirmed dementias: a voxelwise analysis. J Neurol Neurosurg Psychiatry 2017;88:908-916.
33. Zeighami Y, Fereshtehnejad SM, Dadar M, et al. A clinical-anatomical signature of Parkinson's disease identified with partial least squares and magnetic resonance imaging. Neuroimage 2019;190:69-78.
34. Parkinson Progression Marker I. The Parkinson Progression Marker Initiative (PPMI). Prog Neurobiol 2011;95:629-635.
35. Kalra S, Khan M, Barlow L, et al. The Canadian ALS Neuroimaging Consortium (CALSNIC) - a multicentre platform for standardized imaging and clinical studies in ALS. medRxiv, 2020.
36. Aubert-Broche B, Fonov VS, Garcia-Lorenzo D, et al. A new method for structural volume analysis of longitudinal brain MRI data and its application in studying the growth trajectories of anatomical brain structures in childhood. Neuroimage 2013;82:393-402.
37. Ashburner J, Friston KJ. Voxel-based morphometry--the methods. Neuroimage 2000;11:805-821.
38. Fonov V, Evans AC, Botteron K, Almli CR, McKinstry RC, Collins DL. Unbiased average age-appropriate atlases for pediatric studies. Neuroimage 2011;54:313-327.
39. Shen EH, Overly CC, Jones AR. The Allen Human Brain Atlas: comprehensive gene expression mapping of the human brain. Trends Neurosci 2012;35:711-714.
40. Gryglewski G, Seiger R, James GM, et al. Spatial analysis and high resolution mapping of the human whole-brain transcriptome for integrative analysis in neuroimaging. Neuroimage 2018;176:259-267.
41. McKenzie AT, Wang M, Hauberg ME, et al. Brain Cell Type Specific Gene Expression and Co-expression Network Architectures. Sci Rep 2018;8:8868.
42. Tzourio-Mazoyer N, Landeau B, Papathanassiou D, et al. Automated anatomical labeling of activations in SPM using a macroscopic anatomical parcellation of the MNI MRI single-subject brain. Neuroimage 2002;15:273-289.
43. Desikan RS, Ségonne F, Fischl B, et al. An automated labeling system for subdividing the human cerebral cortex on MRI scans into gyral based regions of interest. Neuroimage 2006;31:968-980.

44. Li J, Pan L, Pembroke WG, et al. Conservation and divergence of vulnerability and responses to stressors between human and mouse astrocytes. Nat Commun 2021;12:3958.
45. González-Reyes RE, Nava-Mesa MO, Vargas-Sánchez K, Ariza-Salamanca D, Mora-Muñoz L. Involvement of Astrocytes in Alzheimer's Disease from a Neuroinflammatory and Oxidative Stress Perspective. Front Mol Neurosci 2017;10:427.
46. Preininger MK, Kaufer D. Blood-Brain Barrier Dysfunction and Astrocyte Senescence as Reciprocal Drivers of Neuropathology in Aging. Int J Mol Sci 2022;23.
47. Yang P, Min X-L, Mohammadi M, et al. Endothelial Degeneration of Parkinson's Disease is Related to Alpha-Synuclein Aggregation. Journal of Alzheimer's Disease & Parkinsonism 2017;7.
48. Salmina AB, Inzhutova AI, Malinovskaya NA, Petrova MM. Endothelial dysfunction and repair in Alzheimer-type neurodegeneration: neuronal and glial control. J Alzheimers Dis 2010;22:17-36.
49. Kalaria RN. Cerebrovascular degeneration is related to amyloid-beta protein deposition in Alzheimer's disease. Ann N Y Acad Sci 1997;826:263-271.
50. Procter TV, Williams A, Montagne A. Interplay between Brain Pericytes and Endothelial Cells in Dementia. Am J Pathol 2021;191:1917-1931.
51. Geloso MC, Corvino V, Marchese E, Serrano A, Michetti F, D'Ambrosi N. The Dual Role of Microglia in ALS: Mechanisms and Therapeutic Approaches. Front Aging Neurosci 2017;9:242.
52. Malpetti M, Jones PS, Hezemans FH, et al. Microglial activation and atrophy in frontal cortex predict executive dysfunction in frontotemporal dementia. Alzheimer's & Dementia 2022;17.
53. Perea JR, Llorens-Martin M, Avila J, Bolos M. The Role of Microglia in the Spread of Tau: Relevance for Tauopathies. Front Cell Neurosci 2018;12:172.
54. Keren-Shaul H, Spinrad A, Weiner A, et al. A Unique Microglia Type Associated with Restricting Development of Alzheimer's Disease. Cell 2017;169:1276-1290 e1217.
55. Vandenbark AA, Offner H, Matejuk S, Matejuk A. Microglia and astrocyte involvement in neurodegeneration and brain cancer. J Neuroinflammation 2021;18:298.
56. Zhou Y, Song WM, Andhey PS, et al. Human and mouse single-nucleus transcriptomics reveal TREM2-dependent and TREM2-independent cellular responses in Alzheimer's disease. Nat Med 2020;26:131-142.
57. Hu Y, Fryatt GL, Ghorbani M, et al. Replicative senescence dictates the emergence of disease-associated microglia and contributes to Abeta pathology. Cell Rep 2021;35:109228.
58. Streit WJ, Khoshbouei H, Bechmann I. Dystrophic microglia in late-onset Alzheimer's disease. Glia 2020;68:845-854.
59. Balusu S, Praschberger R, Lauwers E, De Strooper B, Verstreken P. Neurodegeneration cell per cell. Neuron 2023.
60. Lau V, Ramer L, Tremblay M. An aging, pathology burden, and glial senescence build-up hypothesis for late onset Alzheimer's disease. Nat Commun 2023;14:1670.
61. Armada-Moreira A, Ribeiro FF, Sebastião AM, Xapelli S. Neuroinflammatory modulators of oligodendrogenesis. Neuroimmunology and Neuroinflammation 2015;2:263-273.
62. Mot AI, Depp C, Nave KA. An emerging role of dysfunctional axon-oligodendrocyte coupling in neurodegenerative diseases. Dialogues Clin Neurosci 2018;20:283-292.
63. Bryois J, Skene NG, Hansen TF, et al. Genetic identification of cell types underlying brain complex traits yields insights into the etiology of Parkinson's disease. Nat Genet 2020;52:482-493.
64. Feleke R, Reynolds RH, Smith AM, et al. Cross-platform transcriptional profiling identifies common and distinct molecular pathologies in Lewy body diseases. Acta Neuropathol 2021;142:449-474.
65. Agarwal D, Sandor C, Volpato V, et al. A single-cell atlas of the human substantia nigra reveals cell-specific pathways associated with neurological disorders. Nat Commun 2020;11:4183.

66. Orimo S, Uchihara T, Kanazawa T, et al. Unmyelinated axons are more vulnerable to degeneration than myelinated axons of the cardiac nerve in Parkinson's disease. Neuropathol Appl Neurobiol 2011;37:791-802.
67. Wakabayashi K, Hayashi S, Yoshimoto M, Kudo H, Takahashi H. NACP/alpha-synuclein-positive filamentous inclusions in astrocytes and oligodendrocytes of Parkinson's disease brains. Acta Neuropathol 2000;99:14-20.
68. Palhol JSC, Balia M, Terán FS-R, Labarchède M, Gontier E, Battefeld A. A population of gray matter oligodendrocytes directly associates with the vasculature. bioRxiv preprint 2022.
69. Arai K, Lo EH. An oligovascular niche: cerebral endothelial cells promote the survival and proliferation of oligodendrocyte precursor cells. J Neurosci 2009;29:4351-4355.
70. Mathys H, Davila-Velderrain J, Peng Z, et al. Single-cell transcriptomic analysis of Alzheimer's disease. Nature 2019;570:332-337.
71. Ohtomo R, Iwata A, Arai K. Molecular Mechanisms of Oligodendrocyte Regeneration in White Matter-Related Diseases. Int J Mol Sci 2018;19.
72. Traiffort E, Morisset-Lopez S, Moussaed M, Zahaf A. Defective Oligodendroglial Lineage and Demyelination in Amyotrophic Lateral Sclerosis. Int J Mol Sci 2021;22.
73. Spaas J, van Veggel L, Schepers M, et al. Oxidative stress and impaired oligodendrocyte precursor cell differentiation in neurological disorders. Cell Mol Life Sci 2021;78:4615-4637.
74. Heo D, Ling JP, Molina-Castro GC, et al. Stage-specific control of oligodendrocyte survival and morphogenesis by TDP-43. Elife 2022;11.
75. Wang J, Ho WY, Lim K, et al. Cell-autonomous requirement of TDP-43, an ALS/FTD signature protein, for oligodendrocyte survival and myelination. Proc Natl Acad Sci U S A 2018;115:E10941-e10950.
76. Kim WS, Kågedal K, Halliday GM. Alpha-synuclein biology in Lewy body diseases. Alzheimers Res Ther 2014;6:73.
77. Howlett DR, Whitfield D, Johnson M, et al. Regional Multiple Pathology Scores Are Associated with Cognitive Decline in Lewy Body Dementias. Brain Pathol 2015;25:401-408.
78. Burton EJ, McKeith IG, Burn DJ, Williams ED, O'Brien JT. Cerebral atrophy in Parkinson's disease with and without dementia: a comparison with Alzheimer's disease, dementia with Lewy bodies and controls. Brain 2004;127:791-800.
79. Mackenzie IR, Rademakers R. The role of transactive response DNA-binding protein-43 in amyotrophic lateral sclerosis and frontotemporal dementia. Curr Opin Neurol 2008;21:693-700.
80. Ferrari R, Kapogiannis D, Huey ED, Momeni P. FTD and ALS: a tale of two diseases. Curr Alzheimer Res 2011;8:273-294.
81. Iturria-Medina Y, Evans AC. On the central role of brain connectivity in neurodegenerative disease progression. Front Aging Neurosci 2015;7:90.
82. Tremblay C, Rahayel S, Vo A, et al. Brain atrophy progression in Parkinson's disease is shaped by connectivity and local vulnerability. Brain Commun 2021;3:fcab269.
83. Zeighami Y, Ulla M, Iturria-Medina Y, et al. Network structure of brain atrophy in de novo Parkinson's disease. Elife 2015;4.
84. Liddelow SA, Guttenplan KA, Clarke LE, et al. Neurotoxic reactive astrocytes are induced by activated microglia. Nature 2017;541:481-487.
85. Yun SP, Kam TI, Panicker N, et al. Block of A1 astrocyte conversion by microglia is neuroprotective in models of Parkinson's disease. Nat Med 2018;24:931-938.
86. Arnatkeviciute A, Fulcher BD, Fornito A. A practical guide to linking brain-wide gene expression and neuroimaging data. Neuroimage 2019;189:353-367.
87. Jackson WS. Selective vulnerability to neurodegenerative disease: the curious case of Prion Protein. Dis Model Mech 2014;7:21-29.

88. Lau SF, Cao H, Fu AKY, Ip NY. Single-nucleus transcriptome analysis reveals dysregulation of angiogenic endothelial cells and neuroprotective glia in Alzheimer's disease. Proc Natl Acad Sci U S A 2020;117:25800-25809.
89. Johnson TS, Xiang S, Dong T, et al. Combinatorial analyses reveal cellular composition changes have different impacts on transcriptomic changes of cell type specific genes in Alzheimer's Disease. Sci Rep 2021;11:353.
90. Wang X, Allen M, Li S, et al. Deciphering cellular transcriptional alterations in Alzheimer's disease brains. Mol Neurodegener 2020;15:38.
91. Nido GS, Dick F, Toker L, et al. Common gene expression signatures in Parkinson's disease are driven by changes in cell composition. Acta Neuropathol Commun 2020;8:55.
92. Zeng H, Huang J, Zhou H, et al. Integrative in situ mapping of single-cell transcriptional states and tissue histopathology in a mouse model of Alzheimer's disease. Nat Neurosci 2023.
93. Grubman A, Chew G, Ouyang JF, et al. A single-cell atlas of entorhinal cortex from individuals with Alzheimer's disease reveals cell-type-specific gene expression regulation. Nat Neurosci 2019;22:2087-2097.
94. Murdock MH, Tsai LH. Insights into Alzheimer's disease from single-cell genomic approaches. Nat Neurosci 2023;26:181-195.
95. Andrade-Moraes CH, Oliveira-Pinto AV, Castro-Fonseca E, et al. Cell number changes in Alzheimer's disease relate to dementia, not to plaques and tangles. Brain 2013;136:3738-3752.
96. Iturria-Medina Y, Hachinski V, Evans AC. The vascular facet of late-onset Alzheimer's disease: an essential factor in a complex multifactorial disorder. Curr Opin Neurol 2017;30:623-629.
97. Iturria-Medina Y, Carbonell FM, Sotero RC, Chouinard-Decorte F, Evans AC, Alzheimer's Disease Neuroimaging I. Multifactorial causal model of brain (dis)organization and therapeutic intervention: Application to Alzheimer's disease. Neuroimage 2017;152:60-77.
98. Iturria-Medina Y, Sotero RC, Toussaint PJ, Mateos-Perez JM, Evans AC, Alzheimer's Disease Neuroimaging I. Early role of vascular dysregulation on late-onset Alzheimer's disease based on multifactorial data-driven analysis. Nat Commun 2016;7:11934.
99. Fonov VS, Dadar M, Manera AL, Ducharme S, Collins L. Clinical subtypes of frontotemporal dementia show different patterns of cortical atrophy. Alzheimer's & Dementia 2021;17.
100. Rosenberg-Katz K, Herman T, Jacob Y, Giladi N, Hendler T, Hausdorff JM. Gray matter atrophy distinguishes between Parkinson disease motor subtypes. Neurology 2013;80:1476-1484.
101. Dai R, Chu T, Zhang M, et al. Evaluating performance and applications of sample-wise cell deconvolution methods on human brain transcriptomic data. bioRxiv 2023.
102. Iturria-Medina Y, Khan AF, Adewale Q, Shirazi AH, Alzheimer's Disease Neuroimaging I. Blood and brain gene expression trajectories mirror neuropathology and clinical deterioration in neurodegeneration. Brain 2020;143:661-673.
103. Hammond TR, Dufort C, Dissing-Olesen L, et al. Single-Cell RNA Sequencing of Microglia throughout the Mouse Lifespan and in the Injured Brain Reveals Complex Cell-State Changes. Immunity 2019;50:253-271.e256.
104. Jaffe AE, Tao R, Norris AL, et al. qSVA framework for RNA quality correction in differential expression analysis. Proc Natl Acad Sci U S A 2017;114:7130-7135.
105. Yu X, Abbas-Aghababazadeh F, Chen YA, Fridley BL. Statistical and Bioinformatics Analysis of Data from Bulk and Single-Cell RNA Sequencing Experiments. Methods Mol Biol 2021;2194:143-175.
106. Whitwell JL. Voxel-based morphometry: an automated technique for assessing structural changes in the brain. J Neurosci 2009;29:9661-9664.
107. Chung MK, Worsley KJ, Paus T, et al. A unified statistical approach to deformation-based morphometry. Neuroimage 2001;14:595-606.

108. Dadar M, Manera AL, Zinman L, et al. Cerebral atrophy in amyotrophic lateral sclerosis parallels the pathological distribution of TDP43. Brain Commun 2020;2:fcaa061.
109. Dadar M, Manera AL, Ducharme S, Collins DL. White matter hyperintensities are associated with grey matter atrophy and cognitive decline in Alzheimer's disease and frontotemporal dementia. Neurobiol Aging 2022;111:54-63.

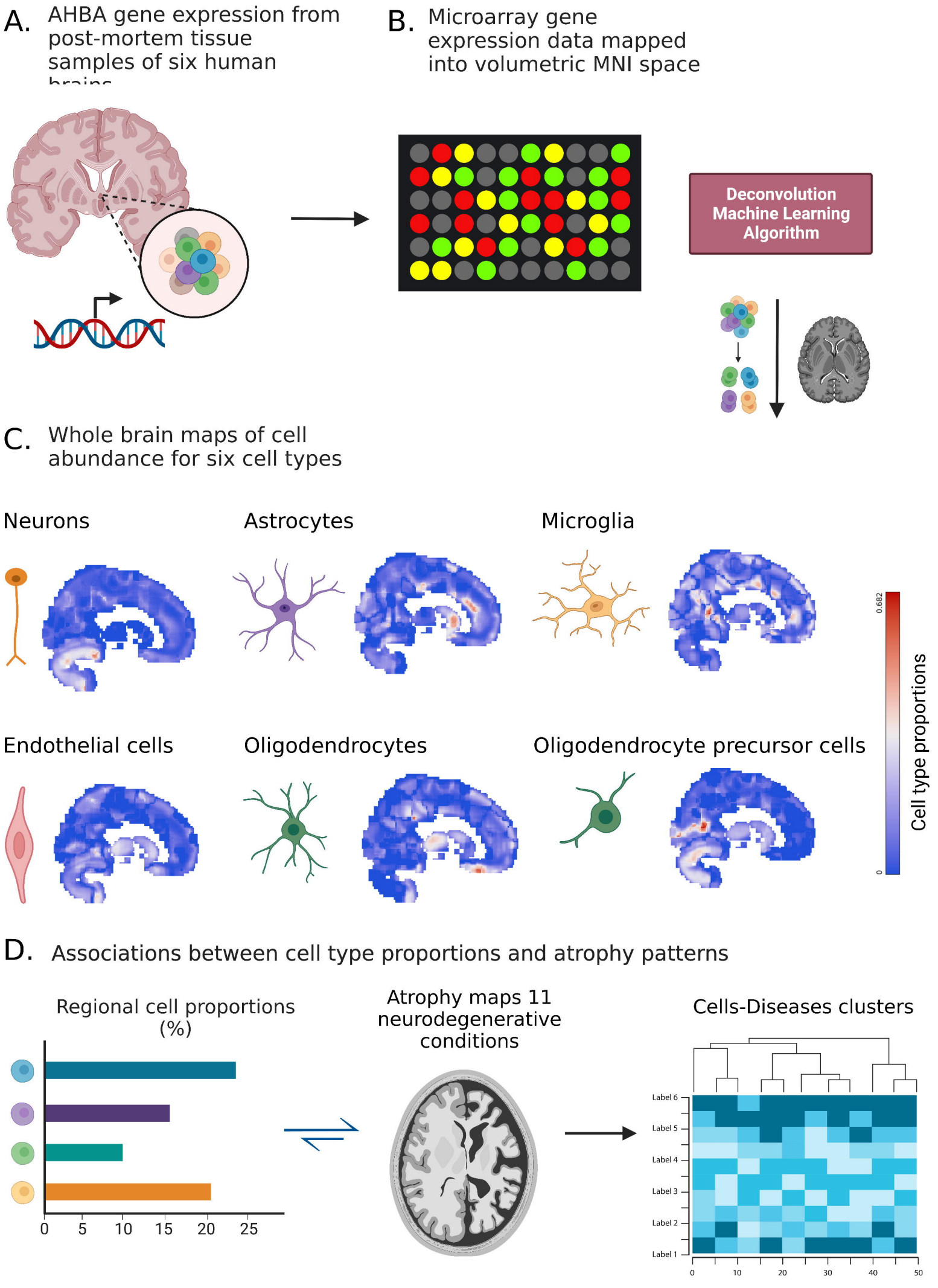
A.
AHBA gene expression from post-mortem tissue samples of six human brains
B.
Microarray gene expression data mapped into volumetric MNI space
Deconvolution Machine Learning Algorithm
C.
Whole brain maps of cell abundance for six cell types
Neurons
Astrocytes
Microglia
Endothelial cells
Oligodendrocytes
Oligodendrocyte precursor cells
0.682
0
Cell type proportions
D.
Associations between cell type proportions and atrophy patterns
Regional cell proportions (%)
0
5
10
15
20
25
Atrophy maps 11 neurodegenerative conditions
Cells-Diseases clusters
Label 6
Label 5
Label 4
Label 3
Label 2
Label 1
0
10
20
30
40
50

Correspondence between tissue integrity and cell density in 118 GM regions

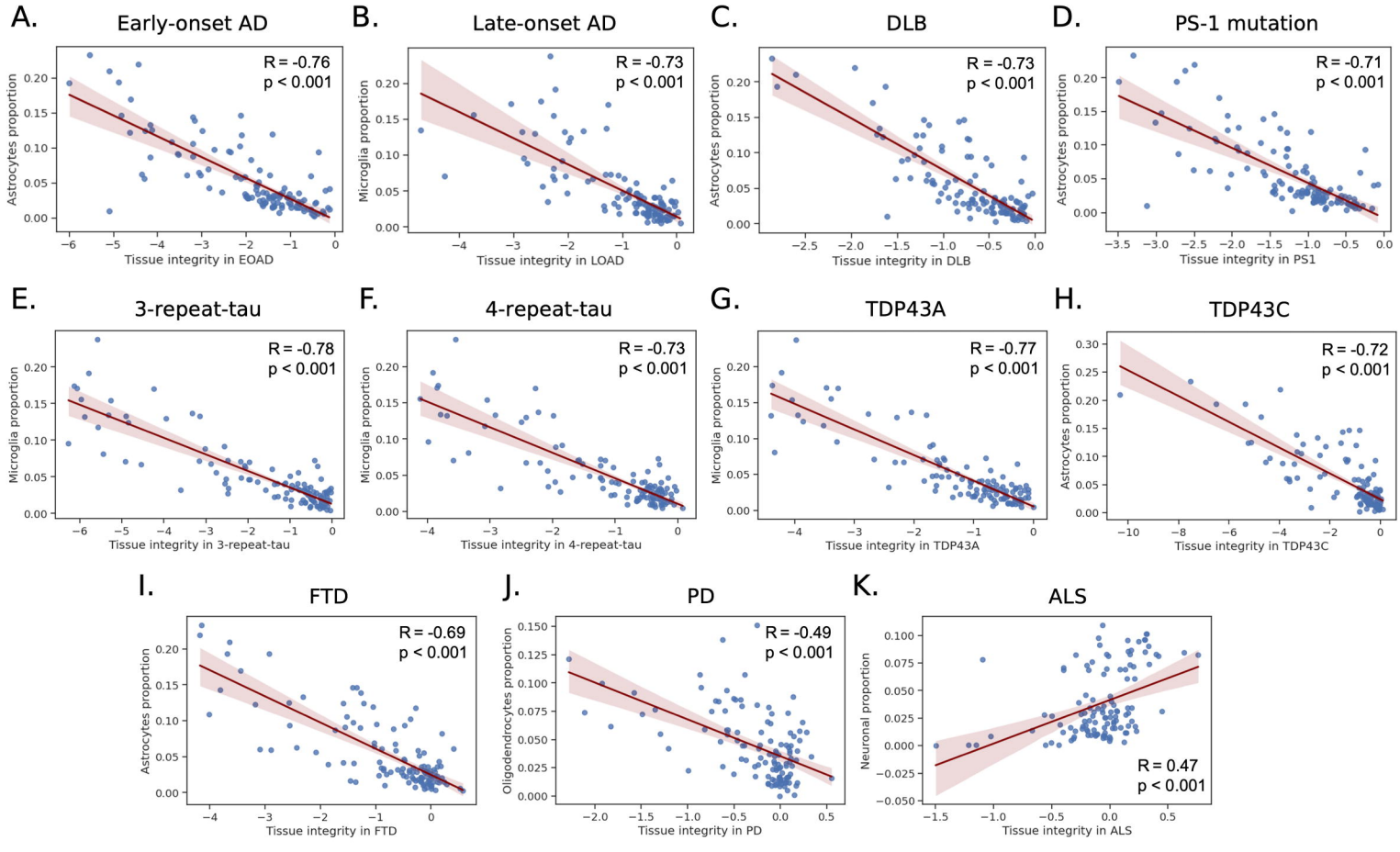

L.

Spearman's correlation coefficients for cells and diseases

	EOAD	LOAD	PS1	3RTau	4RTau	DLB	TDP43A	TDP43C	PD	FTD	ALS
astrocytes	-0.759	-0.708	-0.727	-0.682	-0.712	-0.715	-0.725	-0.717	-0.453	-0.686	0.042
endothelial cells	-0.523	-0.38	-0.496	-0.498	-0.556	-0.487	-0.559	-0.544	-0.306	-0.571	0.048
microglia	-0.718	-0.73	-0.724	-0.783	-0.73	-0.71	-0.773	-0.679	-0.434	-0.679	0.148
neurons	-0.307	-0.258	-0.318	-0.352	-0.287	-0.483	-0.345	-0.291	0.064	-0.119	0.471
oligodendrocytes	-0.585	-0.538	-0.642	-0.657	-0.673	-0.59	-0.67	-0.608	-0.492	-0.522	0.032
OPC	-0.366	-0.318	-0.381	-0.304	-0.311	-0.495	-0.348	-0.405	-0.229	-0.16	0.29

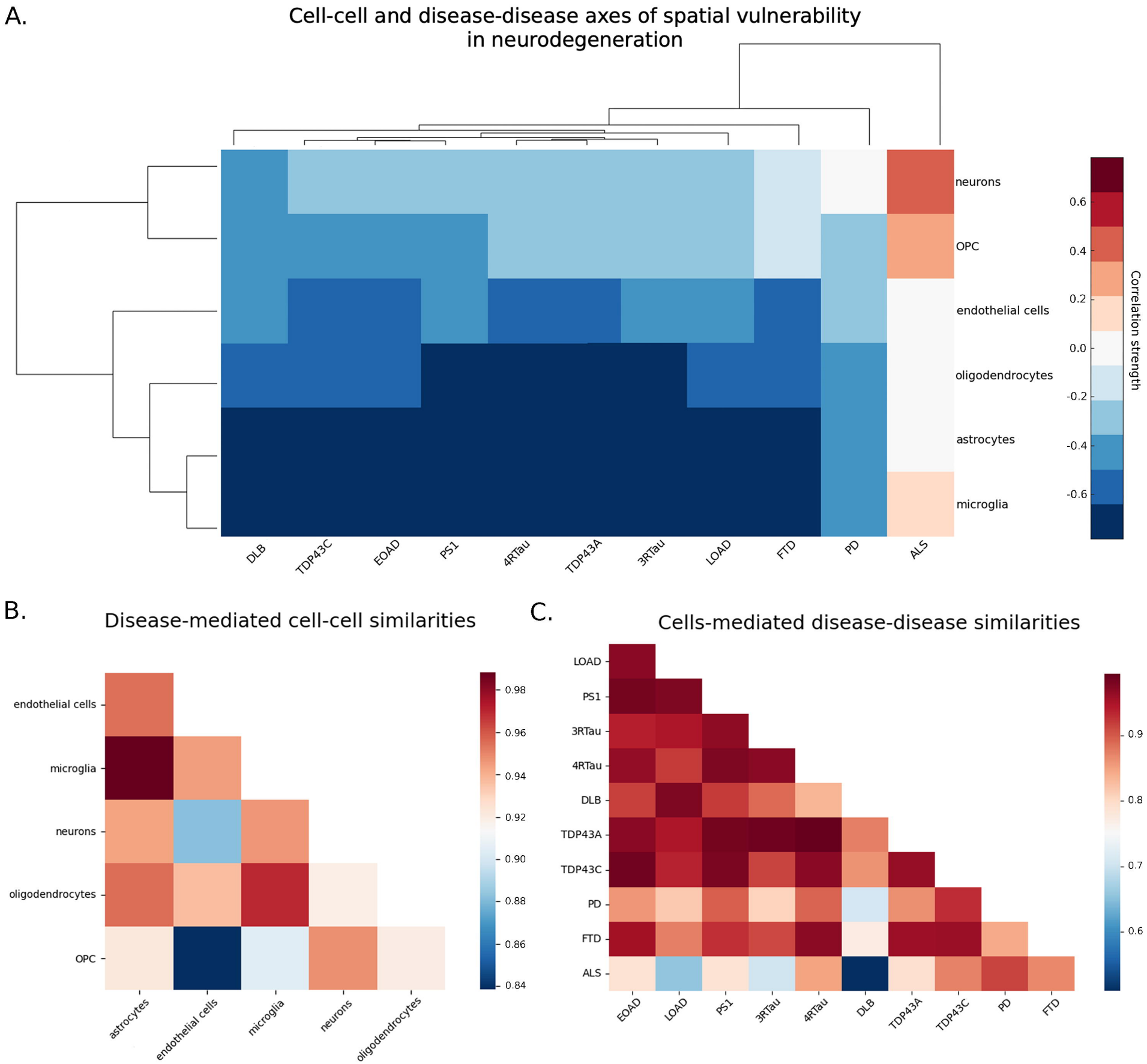
A.
Cell-cell and disease-disease axes of spatial vulnerability in neurodegeneration
neurons
OPC
endothelial cells
oligodendrocytes
astrocytes
microglia
DLB
TDP43C
EOAD
PS1
4RTau
TDP43A
3RTau
LOAD
FTD
PD
ALS
Correlation strength
0.6
0.4
0.2
0.0
-0.2
-0.4
-0.6
B.
Disease-mediated cell-cell similarities
endothelial cells
microglia
neurons
oligodendrocytes
OPC
astrocytes
endothelial cells
microglia
neurons
oligodendrocytes
0.98
0.96
0.94
0.92
0.90
0.88
0.86
0.84
C.
Cells-mediated disease-disease similarities
LOAD
PS1
3RTau
4RTau
DLB
TDP43A
TDP43C
PD
FTD
ALS
EOAD
LOAD
PS1
3RTau
4RTau
DLB
TDP43A
TDP43C
PD
FTD
0.9
0.8
0.7
0.6